SCALING THE VERTICAL STRUCTURE OF SEA BREEZES

D.G. STEYN
Atmospheric Science Programme, Department of Geography The University of British Columbia Vancouver, B.C. Canada

(Received in final form 31 October, 1997)

Abstract. This analysis presents a new set of scalings for sea-breeze circulations. The scales are based on surface-layer turbulent fluxes of sensible heat and momentum, thus avoiding the use of exchange coefficients. Nondimensionalization of the governing equations, using the new scales, results in four dimensionless governing parameters, two of which are new. A data set consisting of 36 profiles of atmospheric variables during pure sea-breeze circulations is presented. The data are used to generate scaling laws for dimensionless sea-breeze depth and strength in the form of products of powers of the governing dimensionless parameters. These scaling laws are used to nondimensionalize individual velocity profiles, which are composited to present a universal dimensionless sea-breeze velocity profile. The scaling laws, applied as a diagnostic scheme, are used to investigate the diurnal evolution of the depth and strength of sea breezes.

Keywords: Sea breeze, Scaling laws, Dimensionless profiles

1. Introduction

Because of their importance to human affairs and their fascinating dynamics, sea breezes have been the subject of study by meteorologists for many years (Jehn, 1973). Thanks to ease of measurement by near surface networks of instruments, observational studies have concentrated on the horizontal structure, thus revealing much about the timing, horizontal extent, strength and wind fields within sea breezes (Atkinson, 1981; Hsu, 1988; Simpson, 1994). There exist many studies of the depth of sea-breeze layers (summarized by Atkinson, 1981), a few fixed site lidar studies of sea-breeze flow structures (Intieri, 1990) and a notable lidar study of the structure of sea-breeze fronts (Nakane and Sasano, 1986). What is known about the vertical structure of sea breezes is confined to pilot balloon measurements of wind speed ranging from the early study of Fisher (1960) to the recent work of Oliphant (1996). These latter works present vertical sections as well as profiles, but the data are coarsely resolved, and do not allow analysis in any detail of the wind profile shape. Also notable, though with lesser vertical resolution, are the aircraft based studies of sea breezes in South Australia typified by Finkele et al. (1995). Analytical modelling studies ranging from the early work of Schmidt (1947) to the recent work of Feliks (1994) employing varying degrees of linearization explore many aspects of the sea breeze, including wind profile shape. These studies are ultimately limited by the extent of linearization needed to render the equations

Boundary-Layer Meteorology **86:** 505–524, 1998.

soluble. Numerical modelling studies (for example Miao and Steyn, 1995) are able to reveal vertically resolved flow structures within sea breezes, but often lack data of sufficient resolution to verify model results.

The objectives of this paper are to investigate the vertical structure (velocity profile) of sea breezes using a set of very high vertical resolution (generally less than 10 metres) observed profiles of wind speed, wind direction, temperature and vapour pressure from one location. Since the work will rely on a number of profiles collected on different days at varying distances from the coastline, the data will be presented as nondimensionalized profiles. In order to perform this nondimensionalization, a new set of scalings for sea breezes will be developed. The scalings will be applied to the data in order to devise scaling laws for the strength and depth of the sea breeze. These scaling laws will then be applied to individual profiles in order to render them dimensionless. A composite dimensionless profile will be developed. The scaling laws will be used as diagnostic tools to investigate the diurnal evolution of the vertical structure of sea breezes, using smoothed, ensemble averaged values for governing variables.

2. Sea Breeze Scalings

The sequence of analytical studies mentioned earlier contains the works of Walsh (1974), Kimura and Eguchi (1978), Ueda (1983) and Niino (1987). All of these studies start the analysis by nondimensionalizing the governing equations. This is achieved by a selected set of scales for all variables in the problem. The scales are devised from external or governing parameters. The governing equations under the Boussinesq approximation are:

$$\frac{\partial u}{\partial t} + u\frac{\partial u}{\partial x} - fv = -\frac{1}{\rho}\frac{\partial p}{\partial x} - \frac{\partial}{\partial z}\overline{w'u'} \tag{2.1}$$

$$\frac{\partial v}{\partial t} + u\frac{\partial v}{\partial x} + fu = -\frac{1}{\rho}\frac{\partial p}{\partial y} - \frac{\partial}{\partial z}\overline{w'v'} \tag{2.2}$$

$$\frac{\partial w}{\partial t} + u\frac{\partial w}{\partial x} = -\frac{1}{\rho}\frac{\partial p}{\partial z} - \frac{\partial}{\partial z}(\overline{w'w'}) + \frac{g}{T_0}T \tag{2.3}$$

$$\frac{g}{T_0}\frac{\partial T}{\partial t} + \frac{ug}{T_0}\frac{\partial T}{\partial x} + N^2 w = -\frac{g}{T_0}\frac{\partial}{\partial z}\overline{w'T'} \tag{2.4}$$

$$\frac{\partial u}{\partial x} + \frac{\partial w}{\partial z} = 0. \tag{2.5}$$

The set of five internal variables is:

$$\left\{u, v, w, T, \frac{p}{\rho}\right\},$$

while the set of seven external or forcing variables is

$$\left\{M, H, \Delta T, N, \frac{g}{T_0}, f, \omega\right\}.$$

Given that the system is expressed in terms of three fundamental dimensional units, (length, time and temperature) there can be only four independent dimensionless governing parameters. In the above, M is the surface layer kinematic momentum flux given by $M = [(\overline{w'u'})^2 + (\overline{w'v'})^2]^{1/2}$, H is the surface layer kinematic sensible heat flux given by $H = \overline{w'T'}$, $N = \sqrt{g\Gamma/T_0}$ is the Brunt-Vaisala frequency where Γ is the mean environmental gradient of potential temperature ($\partial v/\partial z$) of the surrounding atmosphere, ΔT is the land-sea temperature difference, f is the Coriolis parameter and ω is the period of diurnal heating. Other variables are conventionally defined. Equations (2.1) to (2.5) are to be rendered dimensionless by employing appropriately chosen scales for all quantities involved.

In their analyses, Walsh (1974), Kimura and Eguchi, (1978), Ueda (1983), and Niino (1987), invoke first-order closure to eliminate eddy correlation terms in Equations (2.1) to (2.5), and specify constant eddy diffusivities. The use of eddy diffusivities to represent vertical transport of heat and momentum is inappropriate in studies of the sea-breeze circulation since:

- The eddy diffusivities arise out of a first order turbulence closure that is essentially local. The sea-breeze circulation is of too large a scale to make this a reasonable approach.
- Diffusivities are properties of the flow, and are thus inappropriate as external or forcing variables for the construction of scales.
- One of the assumptions in the studies that take this approach is to specify a constant (height invariant) value for the diffusivities of heat and momentum. This is not in accord with many observational and modelling studies, which show the diffusivities to be strong functions of height.

A much more appropriate (than the eddy diffusivity of heat) forcing variable is the heat (or buoyancy) flux at the surface, since this is what drives the sea-breeze circulation. Table I of Niino (1987) summarizes the scalings used by Walsh (1974), Kimura and Eguchi, (1978) and Ueda (1983) and introduces the Niino (1987) scalings as an outgrowth of, and improvement on the earlier approaches. In order to eliminate the eddy diffusivity of heat from the scalings presented by Niino (1987), one can write a first order closure equation for heat transfer by the whole sea-breeze circulation:

$$\frac{Q_H}{\rho C_p} = K_H \frac{\mathrm{d}T}{\mathrm{d}z} \approx K_H \frac{\Delta T}{z_s} \tag{2.6}$$

where z_s is the vertical length scale and ΔT is the land-sea temperature difference defined earlier. This approximation serves to define a bulk eddy diffusivity by

constructing a vertical temperature gradient appropriate for the whole circulation. Notice that ΔT can also be thought of as the temperature difference across the depth z_s, given a lapse rate of $\Gamma = -\mathrm{d}T/\mathrm{d}z$. K_H can be eliminated from Equation (2.6) using Niino's vertical length scale, $z_s = \sqrt{K_H/\omega}$ to result in a new vertical length scale:

$$z_s = \frac{H}{\omega \Delta T}.$$

profundidad de la brisa en función del calor disponible para impulsar la circulación

Similarly, eliminating K_H from Niino's formulation for horizontal length and pressure scales results in

$$x_s = \frac{NH}{\omega^2 \Delta T}$$

extensión horizontal de la brisa marina (cuánto trabajo hace la flotabilidad para impulsar la brisa contra la atm. estable)

and

$$p_s = \rho \frac{g}{T_0} \frac{H}{\omega}.$$

expansión vertical del aire caliente en la atmósfera inferior

These scales, together with the unchanged horizontal velocity scale

$$u_s = \frac{g \Delta T}{T_0} \frac{1}{N}$$

velocidad horizontal del flujo de la brisa.

used by Walsh (1974), Kimura and Eguchi (1978), Ueda (1983), and Niino (1987) are indicated in Table I for comparison with the scales of Niino (1987). In the data analysis that follows, only scalings for vertical length and horizontal velocity will be needed.

Before moving on to apply these scalings, it is instructive to consider what possible physical interpretations may be attached to each of the scales used. The vertical length scale can be viewed as the vertical flux of heat driving the circulation divided by the average diurnal heating rate (represented by $\omega \Delta T$). This ratio should obviously be a measure of the vertical extent of the circulation. Given this interpretation, the horizontal length scale is clearly an aspect ratio (N/ω) multiplied by the vertical length scale. An interpretation of the horizontal velocity scale can be arrived at by considering the rate of work done by buoyancy in driving the sea-breeze flow against the stable, surrounding atmosphere. This rate must be inversely related to N, and directly related to the buoyancy excess represented by the land-sea temperature difference ($g \Delta T / T_0$). The pressure scale can be thought of as the buoyancy excess multiplied by the vertical length scale (ΔT cancelling), since it is by buoyancy forced relative vertical expansion of the lower atmosphere that the horizontal pressure gradients driving a sea breeze are established. These considerations are important in justifying the scalings since any rational scaling must represent underlying physical processes.

TABLE I

Sea breeze scaling used by Niino (1987) and proposed in the present analysis. Vertical length and horizontal velocity scalings are shown because they are central to the present analysis. Horizontal length and pressure scalings are shown because these two are changed from Niino's scheme by the suggested elimination of K_H

Author	Vertical length	Horizontal velocity	Horizontal length	Pressure
Niino (1987)	$\left(\frac{K_H}{\omega}\right)^{1/2}$	$\frac{g\Delta T}{T_0}\frac{1}{N}$	$\frac{N}{\omega}\left(\frac{K_H}{\omega}\right)^{1/2}$	$\rho\frac{g\Delta T}{T_0}\left(\frac{K_H}{\omega}\right)^{1/2}$
Steyn	$\frac{H}{\omega\Delta T}$	$\frac{g\Delta T}{T_0}\frac{1}{N}$	$\frac{NH}{\omega^2\Delta T}$	$\rho\frac{g}{T_0}\frac{H}{\omega}$

In addition to the scales listed in Table I, heat flux is scaled by H, momentum flux by M, and (following Niino, 1987) vertical velocity is scaled by $g\Delta T\omega/T_0N^2$, time by $1/\omega$, and temperature by ΔT. Nondimensionalization transforms Equations (2.1) to (2.6) to:

$$\frac{\partial u^*}{\partial t^*}+\frac{\Pi_1}{\Pi_4}u^*\frac{\partial u^*}{\partial x^*}-\Pi_2 v^*=-\frac{\partial p^*}{\partial x^*}-\Pi_3\frac{\partial}{\partial z^*}(\overline{w'u'})^* \tag{2.7}$$

$$\frac{\partial v^*}{\partial t^*}+\frac{\Pi_1}{\Pi_4}u^*\frac{\partial v^*}{\partial x^*}+\Pi_2 u^*=-\frac{\partial p^*}{\partial y^*}-\Pi_3\frac{\partial}{\partial z^*}(\overline{w'v'})^* \tag{2.8}$$

$$\frac{\partial w^*}{\partial t^*}+\frac{\Pi_1}{\Pi_4}u^*\frac{\partial w^*}{\partial x^*}=-\Pi_4^2\frac{\partial p^*}{\partial z^*}-\Pi_3\Pi_4\frac{\partial}{\partial z^*}(\overline{w'w'})^*+\Pi_4^2T^* \tag{2.9}$$

$$\frac{\partial T^*}{\partial t^*}+\frac{\Pi_1}{\Pi_4}u^*\frac{\partial T^*}{\partial x^*}+w^*=-\frac{\partial}{\partial z^*}(\overline{w'T'})^* \tag{2.10}$$

$$\frac{\partial u^*}{\partial x^*}+\frac{\partial w^*}{\partial z^*}=0. \tag{2.11}$$

All starred quantities are dimensionless, and the four dimensionless governing parameters (Π_1 to Π_4) are: $\Pi_1=g(\Delta T)^2/T_0NH$, $\Pi_2=f/\omega$, $\Pi_3=T_0MN/gH$ and $\Pi_4=N/\omega$.

The objective of the following section is to search for empirical relations of the form:

$$\frac{\phi_{sb}}{\phi_s}=a\Pi_1^b\Pi_2^c\Pi_3^d\Pi_4^e, \tag{2.12}$$

where ϕ_{sb} is a measured physical property of the sea breeze (in this case, depth and strength), and ϕ_s is the scale appropriate for that quantity.

ppiedad física medida (ej.: prof. brisa)

escala característica de esta ppiedad (ej.: para prof. brisa → z_s)

El comportamiento de cualquier ppiedad física de la brisa marina no depende de las var. dimensionales originales de manera directa sino a través de los par. Π (teoría de similitud de la din. fluidos)

a, b, c, d y e se determinan empíricamente.

3. The Data and their Analysis

Wind profile data giving the vertical structure of sea breezes and a variety of ancillary data are needed to exercise the scalings devised in Section 2.

3.1. PROFILE DATA

As part of a study of meteorological conditions during episodes of ozone pollution in the Lower Fraser Valley (LFV) of British Columbia, tethered balloon measurements were made on a large number of summer days in the years 1983 to 1987. Days for study were chosen on the basis of being forecast to have high temperatures and light winds. The measurement programme involved deploying a tethered balloon under continuous operation from early morning until late evening from a small set of sites (Roberts Bank, Queen Elizabeth Park, Mountain View Cemetery or Burnaby lake) within the valley. Figure 1b indicates these sites, and the coastline. The LFV is a roughly triangular valley spanning the Canada/USA border at 49° N with its westward end being the shoreline of the Strait of Georgia. The open (westward) end of the valley is roughly 100 km in width, of similar dimension to its East/West extent. The valley walls consist of the Coast Mountain Ranges in the north, and the Cascade Ranges in the south. The valley floor is nearly flat, at an elevation of no more than a few hundred metres above sea level, while valley walls to the north rise to 2000 metres above sea level within 10 km of the floor. Walls to the south rise to 1000 metres above sea level.

The instrument employed in these measurements was an Atmospheric Instrumentation Research Inc. model TS-2A tethersonde^{TM} carried aloft by a 4.25 m^3 blimp shaped balloon. In this configuration, wind speed is sensed by a three-arm cup anemometer with a response length of roughly 2 m, wind direction is sensed by the orientation of the balloon while air temperature and wet bulb temperature are sensed by thermistors in a forced aspiration radiation shield. Data were scanned every 10 seconds and telemetered to a recording ground station by radio link. Because of the slow response of the balloon to wind direction changes, the wind signal is subject to considerable errors. Profiles extended up to roughly 1000 m AGL, each taking 20 to 30 minutes to complete, depending on wind speed.

The entire data set consists of 532 individual profiles collected on 26 days during the five summers. A total of 36 profiles taken on 10 days (see Table II for dates) exhibit low level inflow (sea breeze) and upper level outflow (return flow). The criteria for selecting these profiles was that there be a distinct wind speed minimum at the same level as a large wind direction shift. The flow reversal was required to occur over a height of no more than 100 metres. Figure 2 shows a set of profiles measured at 1001 Pacific Standard Time (PST) on 1985.08.23, and is representative of the subset of profiles showing a sea breeze circulation. This figure shows the sea breeze to be roughly 145 m deeper than the thermal internal boundary

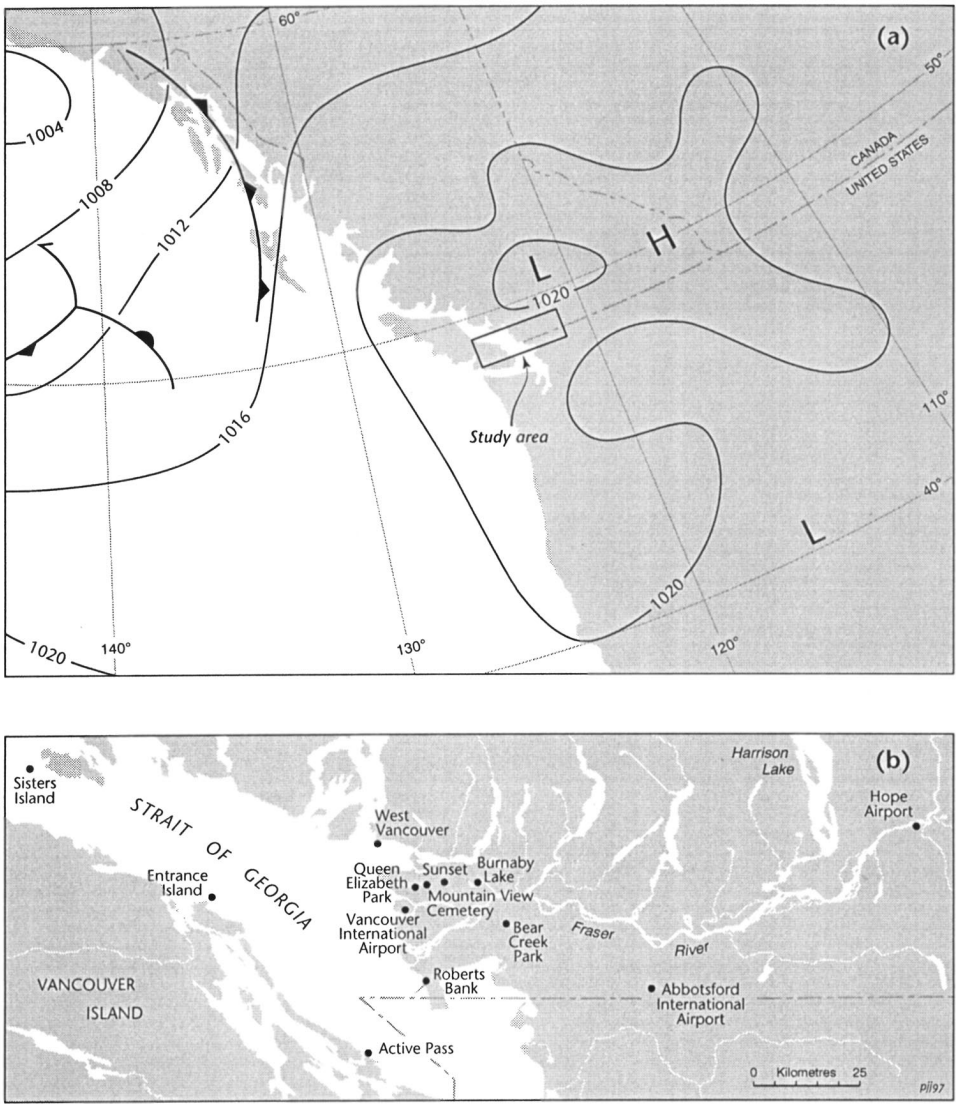

Figure 1. Maps of: (a) The Northeastern Pacific Ocean and Northwestern North America showing synoptic sea level pressure field valid for 1800 UTC (1000 PST) on 1985.08.23. The rectangle marks the area of Figure 1b. (b) The Lower Fraser Valley and Strait of Georgia basin showing all locations referred to in the text.

layer, which is identified by a strong capping potential temperature inversion and fairly sharp reduction in vapour pressure.

All profiles in the subset showed sea breezes to be deeper than or of roughly the same depth as the thermal internal boundary layer. This relationship is governed by relatively shallow thermal internal boundary layers in early morning and close to the shoreline, and the physical impossibility of having a thermal internal boundary

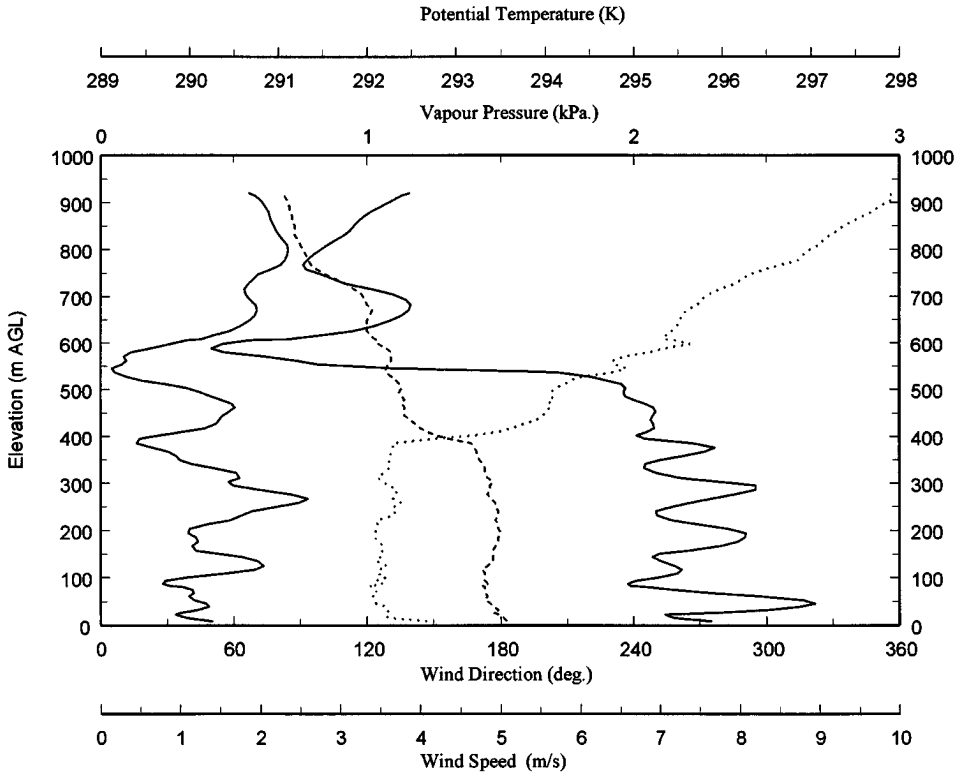

Figure 2. Profiles of wind speed (solid line to left of graph), wind direction (solid line to right of graph), potential temperature (dotted line) and vapour pressure (dashed line) measured at 1001 PST on 1985.08.23. Wind data have been smoothed by application of a seven point, binomially weighted moving average.

layer in the offshore wind of the return flow (Steyn, 1997). It is assumed that this subset of profiles represents steady state, fully developed sea breezes in near-zero synoptic wind. Evidence for this assumption is provided by Figure 1a, which shows the analyzed synoptic scale surface pressure over Southern British Columbia and the adjoining Pacific Ocean at 1000 PST on 23 August, 1985. The pressure field shows a broad, flat anticyclone centered on the LFV, with a small, weak thermal trough lying over the interior of British Columbia. Similarly weak synoptic-scale pressure gradients are present on all days represented in the sea breeze subset of profiles. An examination of the 850 hPa analysed winds over the LFV at 1600 PST on days studied shows very light winds with a preponderance of winds from southerly and easterly sectors.

3.2. ANCILARY DATA

In order to estimate scales for horizontal velocity and vertical length, estimates are needed of the turbulent sensible heat and momentum fluxes (H and M) in the surface layer, the land-sea temperature difference (ΔT), the environmental gradient of potential temperature (Γ) above the thermal internal boundary layer, the base state potential temperature (T_0) and the period of diurnal heating (ω).

3.2.1. *Surface Layer Turbulent Sensible Heat and Momentum Fluxes*

Through much of the field component of this study, a parallel study of urban/rural contrasts in surface energy budgets was conducted by Oke and collaborators. Included in this work was an ongoing programme of measurement of turbulent sensible heat flux from the Sunset site in Vancouver. Details of these measurements are contained in Cleugh and Oke (1986). Measurements of turbulent sensible heat flux as hourly averages were available on all 10 days reported in Table II. These data were interpolated to provide heat flux values midway through each of the measured profiles. No directly measured momentum fluxes are available. This quantity may be estimated to reasonable precision using measured wind speed, measured heat flux, and estimated surface roughness length (from land use) via the Monin-Obukhov similarity theory.

3.2.2. *Land-Sea Temperature Difference*

The detailed definition of this variable is a matter that could be debated at length. In the present study, T_{sea} is taken to be a representative sea water surface temperature. The body of water which drives the sea breeze circulation in the LFV is the Strait of Georgia (see Figure 1b). The only available measurements of sea surface temperature are bucket measurements taken at lighthouses at Active Pass, Sister's Islands, Entrance Island and West Vancouver (see Figure 1b). These sites are generally subject to strong tidal currents, making measurements representative of relatively large bodies of water. Analyses by Webster and Farmer (1977) show that Strait of Georgia lighthouse data from Active Pass, Sister's Island, Entrance Island and West Vancouver are all representative of water in the Central Strait of Georgia. Based on this conclusion, T_{sea} was taken to be the average of temperatures from these four stations. Table II shows sea surface temperatures from these stations for all 10 days on which sea-breeze profiles are available.

Hourly screen-height air temperature is taken as an operational definition of T_{land}. In the coastal zone during sea breezes, screen-height temperature must increase continuously with distance from the shoreline from its over water value through values determined by cool air advection over the near-shore land, to values characteristic of overland air out of influence of the sea breeze. It is clear that the air temperature far from marine influence will be approached asymptotically, and that this asymptote should be substantially reached in fetch distances of at least x_s, the horizontal sea-breeze length scale. Average values of the controlling

TABLE II

Vancouver International Airport (YVR), Abbotsford International Airport (YXX) and Hope Airport (YHE) daily maximum temperatures, Active Pass (AP), Sister's Islands (SI), Entrance Island (EI) and West Vancouver (WV) sea surface temperatures during sea breeze days. Temperatures coded as 99.9 represent missing data. T_{sea} is the average of all available sea temperature data. All temperatures are in °C

		YVR	YXX	YHE	AP	SI	EI	WV	T_{sea}
Jul 22	1983	23.0	27.5	27.3	19.2	19.0	16.2	15.5	17.5
Jul 30	1983	24.8	31.1	30.4	17.8	18.2	17.0	16.1	17.3
Aug 04	1983	22.4	25.7	26.6	18.0	18.5	17.0	99.9	17.7
Aug 05	1983	23.0	23.5	24.3	15.5	18.3	19.1	99.9	17.6
Jul 17	1985	24.1	28.8	28.6	19.8	19.8	19.0	17.8	19.1
Aug 15	1985	25.0	29.8	30.0	16.7	16.9	17.1	15.1	16.5
Aug 23	1985	23.7	31.0	30.5	19.2	17.5	17.1	19.1	18.2
Aug 19	1986	21.9	24.6	28.6	16.4	16.8	17.7	16.8	16.9
Aug 22	1986	24.2	28.4	28.9	16.3	17.0	18.0	15.9	16.8
Aug 26	1986	25.8	33.5	34.3	18.6	18.6	20.0	17.0	18.6

variables in this study result in an x_s of 72 km. Air temperature measurements in the LFV are available at Vancouver International Airport, Abbotsford International Airport and Hope Airport (see Figure 1b) located roughly 5 km, 50 km and 100 km respectively from the shoreline. An analysis of hourly air temperatures at the three airports shows a strong influence of cool marine air advection in that temperatures at Vancouver International Airport are typically lower than the other two temperatures which are generally within two degrees of each other. Table II illustrates this relationship between the daily maximum temperatures on all days in the study. T_{land} is taken as the air temperature at Abbotsford International Airport, interpolated to the time of the profile.

3.2.3. *Environmental Lapse Rate of Potential Temperature*

Values for this forcing variable are extracted from each profile by plotting the profile, and subjectively fitting a straight line to the upper portion of the potential temperature profile. This subjective procedure is chosen because it is important to avoid contaminating the measured lapse rate with temperature profile features determined by inversion base entrainment effects.

3.2.4. *Base State Potential Temperature and Period of Diurnal Heating*

The base state potential temperature is taken as the vertically averaged thermal internal boundary layer potential temperature extracted from the profile data, and the frequency of diurnal heating is $2\pi/24\ \text{hr}^{-1} = 7.272 \times 10^{-5}\ \text{s}^{-1}$.

3.3. ANALYSIS OF DATA

A preliminary check for consistency between profile and sea temperature data was conducted by comparing T_{sea} with the early morning near surface air temperature implied by the fitted upper level profile when extrapolated to sea level. The average difference between these temperatures is -0.2 ± 2.5 K (in the following, $\pm$ will denote a one standard deviation spread), the small average difference being an indication of consistency between the two sources of data. The average ΔT is 7.5 $\pm$ 3.4 K, while the average Γ is 0.0093 ± 0.0047 K m^{-1}.

Wind profile data were averaged vertically in two segments to yield sea breeze (inflow) mean wind direction, speed (given the symbol u_{sb}) and depth (given the symbol z_{sb}) as well as return flow mean wind direction. The two directions are needed to decompose the wind profile into cross-shore and along-shore components. The mean sea-breeze (inflow) wind direction over all profiles was 269 $\pm$ 31 degrees. This is in close agreement with the Vancouver International Airport climatologic mean sea breeze direction of 245 degrees during the hours 1000 to 1700 PST reported by Steyn and Faulkner (1986), while the mean return flow direction was 107 $\pm$ 28 degrees.

3.3.1. *Scaling Laws*

Functional forms of the scaling laws for sea-breeze strength and depth represented by Equation (2.12) cannot be revealed by the dimensional arguments used to derive the scalings, but must be investigated by empirical analysis. Since the present data set is drawn from one location only, $\Pi_2 = f/\omega$ does not vary and its effect cannot be investigated. Ueda (1983), Rotunno (1983) and Niino (1987) show that Π_2 only influences the horizontal dimension of sea breezes, so its constancy is not of significance in the present context. By assuming full similarity of all realizations of the sea breeze circulation, this analysis assumes that there are no fetch (from the shoreline) dependencies in the circulation, and that the circulation is fully adjusted to the surface forcing. This last requirement in effect presumes the easily justifiable assumption that time scales of convection driving the sea breeze are shorter than time scales of the surface-layer diurnal cycle.

The ratio $\sqrt{\Pi_3/\Pi_1}$ is equal to u_{sb}/u_s multiplied by the square root of the Monin-Obukhov function used to estimate M. Since this explicit interdependence of two dimensionless parameters (given specified speed profiles) violates the requirement of independence of all parameters, Π_3 will be excluded from the function specified in Equation (2.12). Π_3, rather than Π_1 is excluded since Π_3 incorporates effects of surface drag which are likely to affect only the lower portion of the sea-breeze profile. By contrast, Π_1 incorporates the effects of convection, which have a much greater influence on vertical structures of the sea breeze.

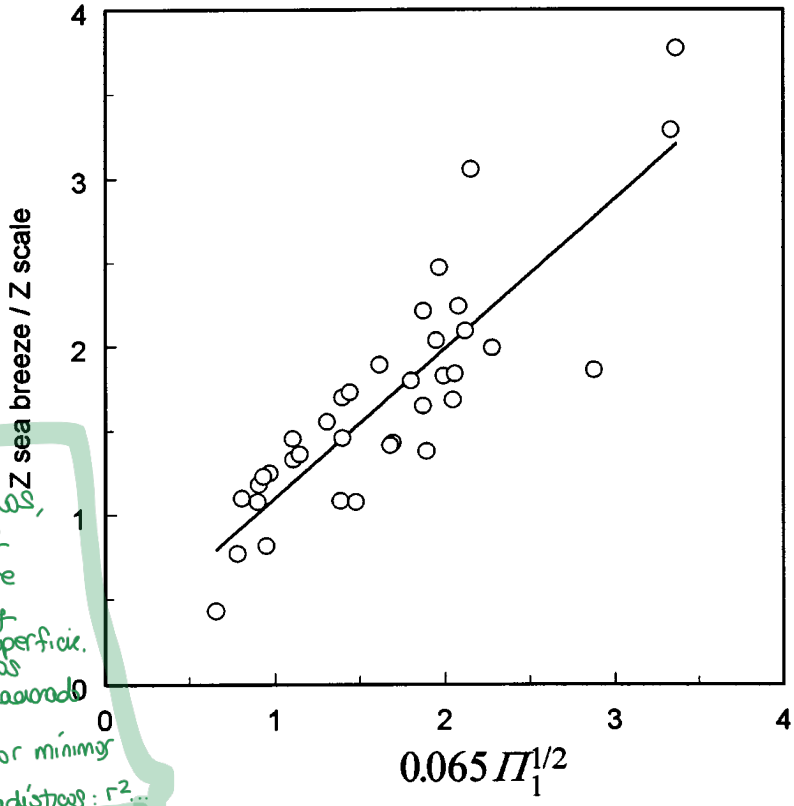

Figure 3. Scatter plot of scaled sea-breeze depth (z_{sb}/z_s) against $0.065\Pi_1^{1/2}$ where $\Pi_1 = g\Delta T^2/T_0 NH$.

Scatter plots show that the scaled sea-breeze depth is unrelated to Π_4, but strongly related to Π_1. Exploratory regression analysis employing non-linear least square fitting procedures shows the best relation between z_{sb}/z_s and Π_1 to be:

$$z_{sb}/z_s = 0.065\Pi_1^{1/2}. \tag{3.1}$$

Figure 3 shows the scatter around the relation (4.1). The standard error of estimate of the coefficient in Equation (3.1) is 0.001, the linear regression coefficient r^2 is 0.73. It is of interest that this equation implies the depth of the sea-breeze circulation to be independent of ΔT.

An analysis similar to that for sea-breeze depth shows u_{sb}/u_s to be closely related to Π_1 and Π_4, with the best relation being:

$$u_{sb}/u_s = 1.10\Pi_1^{-1/2}\Pi_4^{1/4} \tag{3.2}$$

Figure 4 shows the scatter around the (relation 3.2). The standard error of estimate of the coefficient in Equation (3.2) is 0.06, and the linear regression coefficient r^2

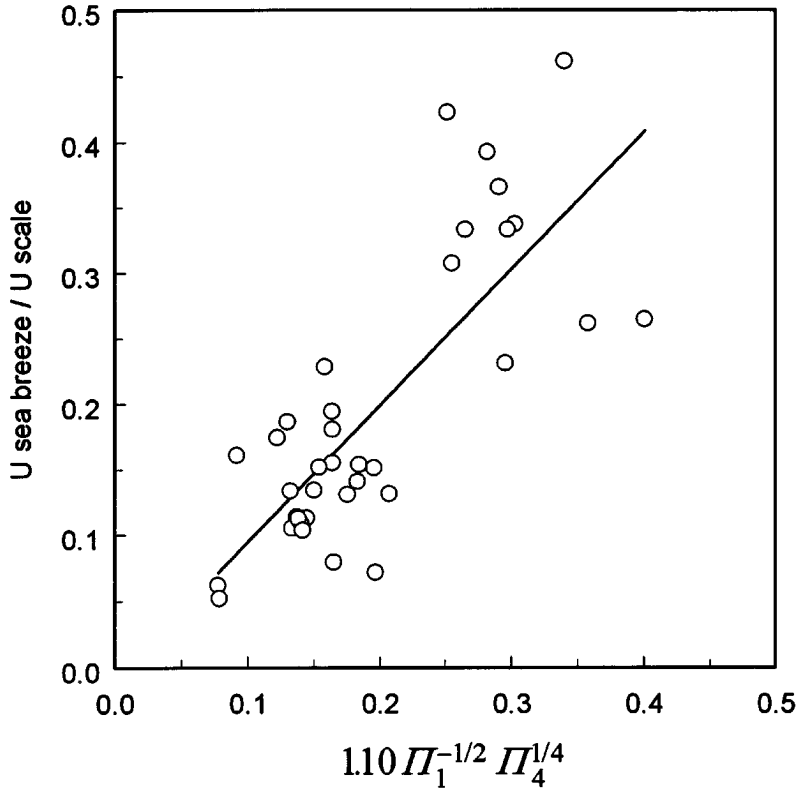

Figure 4. Scatter plot of scaled vertically averaged sea-breeze wind speed (u_{sb}/u_s) against $1.10\Pi_1^{-1/2}\ \Pi_4^{1/4}$, where $\Pi_1 = g\Delta T^2/T_0 NH$ and $\Pi_4 = N/\omega$.

is 0.61. The relatively large scatter in Figure 4 (and to a lesser extent Figure 3) is a result of the relatively large errors in wind profile data mentioned earlier, and the possible influence of dependence on variables not included in the scaling analysis.

An attempt was made to uncover systematic variation in Figures 3 and 4 governed by factors related to date, time of day and location of profile. These analyses show that the data are unable to detect any such systematic variation if it does exist. The possibility of such dependencies cannot be ruled out, given the noisy data. An investigation of the possible effect of non-zero synoptic wind on the velocity scaling was undertaken by plotting deviations from the fitted wind speed relation on Figure 4 against the 850 hPa wind (extracted from 850 hPa weather maps produced by Environment Canada) component parallel to the sea breeze direction. Figure 5 shows the result of this analysis. It is evident from this plot that there is no systematic dependence between the residuals in the velocity scaling law and the 850 hPa wind. Also evident is that the component of the 850 hPa wind parallel to the sea breeze direction is predominantly negative on the days included in this study (indicated by near zero or at most, small negative values). This is not surprising,

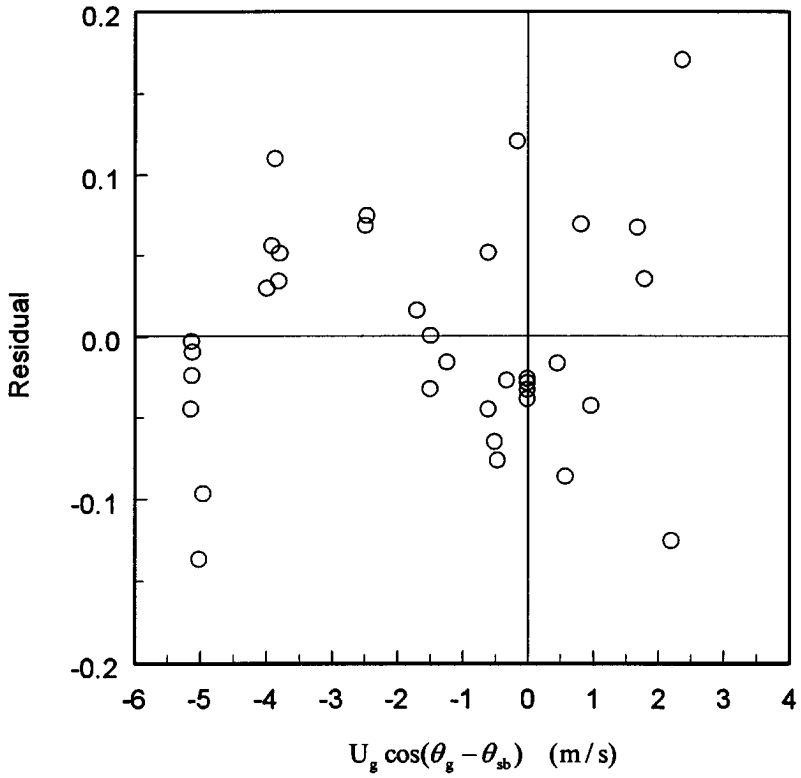

Figure 5. Velocity deviations between fitted velocity scaling law (Equation (3.2)) and individual profile data plotted against 850 hPa wind component parallel to the sea-breeze direction. Residual is $u_{sb} - 1.10\, u_s \Pi_1^{-1/2} \Pi_4^{1/4}$.

since under slight opposing (of the sea breeze) synoptic winds, the return flow would be most evident.

3.3.2. *Composite Profiles*

Given the scaling laws represented by Equations (3.1) and (3.2), the 36 individual profiles can be plotted in dimensionless form on a single set of axes. In order to achieve this, each profile was decomposed into along-shore and cross-shore components using the mean wind directions described earlier. In order to reduce noise in the profiles, components were first smoothed by application of a seven point binomially weighted moving average. Heights AGL were scaled according to Equation (3.1), and velocity components according to Equation (3.2). Each profile was then interpolated (using a cubic spline) to a spacing of 0.02 in scaled height. This spacing was chosen as it coincides roughly with the vertical resolution of the original data. A composite, dimensionless profile was then constructed by averaging scaled velocity at each interpolated, scaled height. The profile of cross-

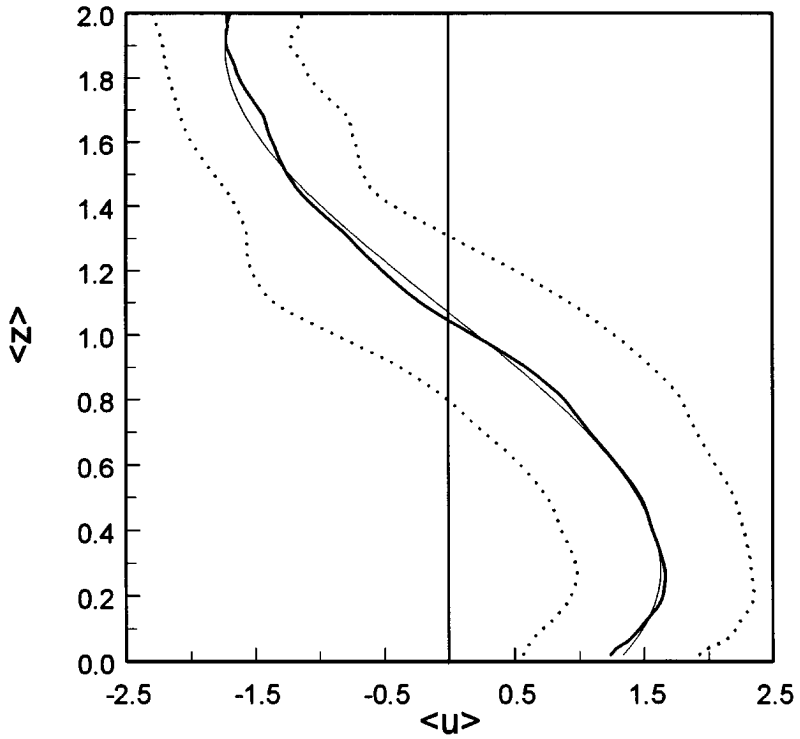

Figure 6. Dimensionless composite profile of cross-shore sea breeze velocity component. The heavy solid line is the mean, dotted lines indicate one standard deviation and the light solid line is the approximating function: $\langle u\rangle = 1.60\langle z\rangle^3 - 5.21\langle z\rangle^2 + 2.54\langle z\rangle + 1.29$, where $\langle u\rangle = u/1.10\Pi_1^{-1/2}\Pi_4^{1/4}$ and $\langle z\rangle = z/0.065\Pi_1^{1/2}$.

shore wind speed, a one standard deviation band and an approximating function are plotted in Figure 6.

The resulting sea-breeze profile is remarkably smooth, shows clearly a velocity minimum near the surface, a low level inflow maximum at a scaled height of 0.26, a velocity zero at roughly 1.04 and a return flow maximum at 1.8. While the one standard deviation band indicates a fair degree of uncertainty, there can be no doubt about the reality of the broad profile features described above. The approximating function is a third order polynomial, and is intended as a basis for comparison with other analyses, rather than an analytical form having physical or mechanistic significance. Figure 7 shows the along-shore component and is intended to indicate (by very small mean values) that the decomposition into along-shore and cross-shore components results in, on average, a cross-shore component that is much larger than the along-shore component shown in Figure 7.

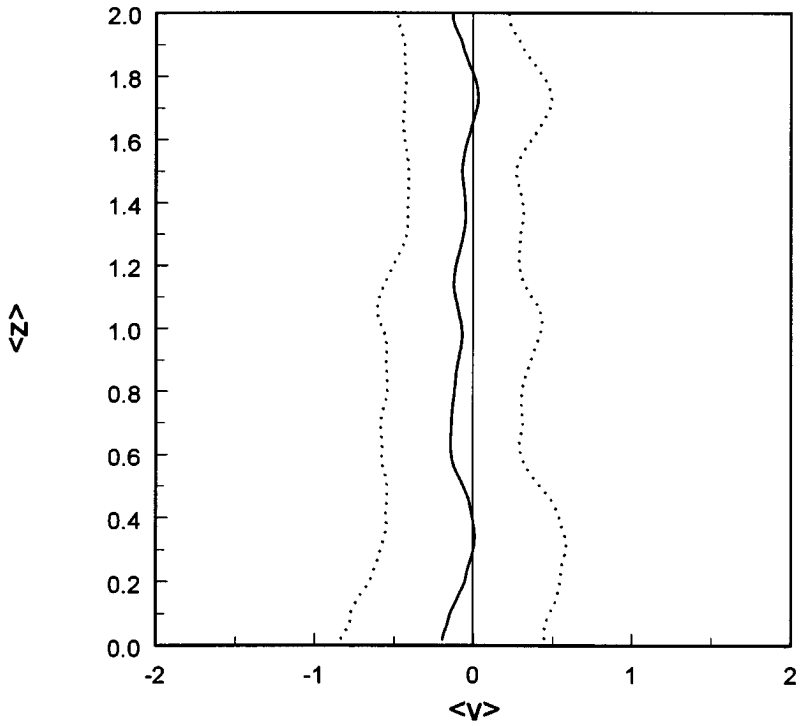

Figure 7. Dimensionless composite profile of along-shore sea breeze velocity component. The solid line is the mean, dotted lines indicate one standard deviation. $\langle v \rangle = v/1.10\Pi_1^{-1/2}\Pi_4^{1/4}$, and $\langle z \rangle = z/0.065\Pi_1^{1/2}$.

4. Discussion and Conclusions

The analysis has resulted in a new set of scalings for sea-breeze circulations, a new set of dimensionless governing parameters for sea-breeze circulations, scaling laws for the depth and strength of sea-breeze circulations, and a universal dimensionless profile for the sea-breeze circulation. The scaling laws and dimensionless profile are derived from observations at one location. While the dimensional analysis captures the essential dynamics of the sea breeze, the results will be strengthened by confirmation that they are consistent with measurements from other locations.

4.1. Scales and scaling laws

The scales derived in this work are an extension of earlier scaling schemes intended as starting points of analytical studies of sea-breeze circulations. The redefined scales with replacement of exchange coefficients by surface-layer turbulent fluxes of sensible heat and momentum as governing variables are preferable since the fluxes are more obvious governing variables than exchange coefficients. In addition, temporal variability of the surface-layer fluxes are better understood, and are

more often measured than exchange coefficients. This temporal variability can be well represented by a small number of Fourier components, thus leading naturally to forcing terms in linear analyses. It is therefore reasonable to speculate that the scalings presented here will be useful starting points for analytical studies. The scales are amenable to seemingly cogent interpretation based on simple physical arguments, and thus appear to be rational ones.

The scaling laws resulting from an application of the scalings to empirical data are subject to some uncertainty because of scatter in the data. Nevertheless, the general form of the scaling laws is well supported. The scaling laws may have dependence on variables not incorporated in this study, though that dependence must remain consistent with the laws presented here. It is possible that the coefficient in Equation (3.2) is dependent on Π_2.

It is entirely possible that the true scaling laws may depend on distance from the coastline. This dependence is likely to be a secondary, and will be resolved only if very high quality data are available. Alternately, mesoscale numerical model output could be employed to investigate this and other dependencies. It is not surprising that the data analyzed in this work represent conditions with synoptic wind components parallel to the return flow with magnitudes from zero to more than double the mean sea-breeze strength. It is only in such conditions that a well developed return flow will be observable. What is of considerable interest is that the present analysis could detect no systematic influence of overlying synoptic flow for this range of wind speeds. It is possible that this dependence, which must surely exist, was buried in scatter in the data. Refinement of the scaling laws can only come through analysis of much higher quality data, or analysis of mesoscale numerical model output.

4.2. DIURNAL EVOLUTION OF THE SEA BREEZE

Since the foregoing analysis results in a set of scales and scaling laws for the depth and strength of sea breezes as functions of governing dimensionless governing parameters, it is possible to examine the diurnal evolution of sea-breeze depth and strength using the scaling laws as a diagnostic scheme. In order to undertake this exercise, the forcing variables H, ΔT, N, T_0 and ω will be given values representative of the present data set. Values for N and T_0 are simply averages of all profile values, 0.017 s^{-1} and 298 K respectively. H, and ΔT are assigned hourly average values based on heavily smoothed ensemble averages from the H and ΔT data sets.

The diurnal evolution of H (multiplied by thermodynamic factors to bring it into thermal units) and ΔT is plotted in the top panel of Figure 8. Of immediate importance is the existence of two transitional periods when H and ΔT have opposite signs, resulting in nonphysical negative values for the scales. These periods represent the transitions between land and sea breezes that occur in the morning (roughly 0645 to 0745 local apparent time in this case) and evening (roughly 2000

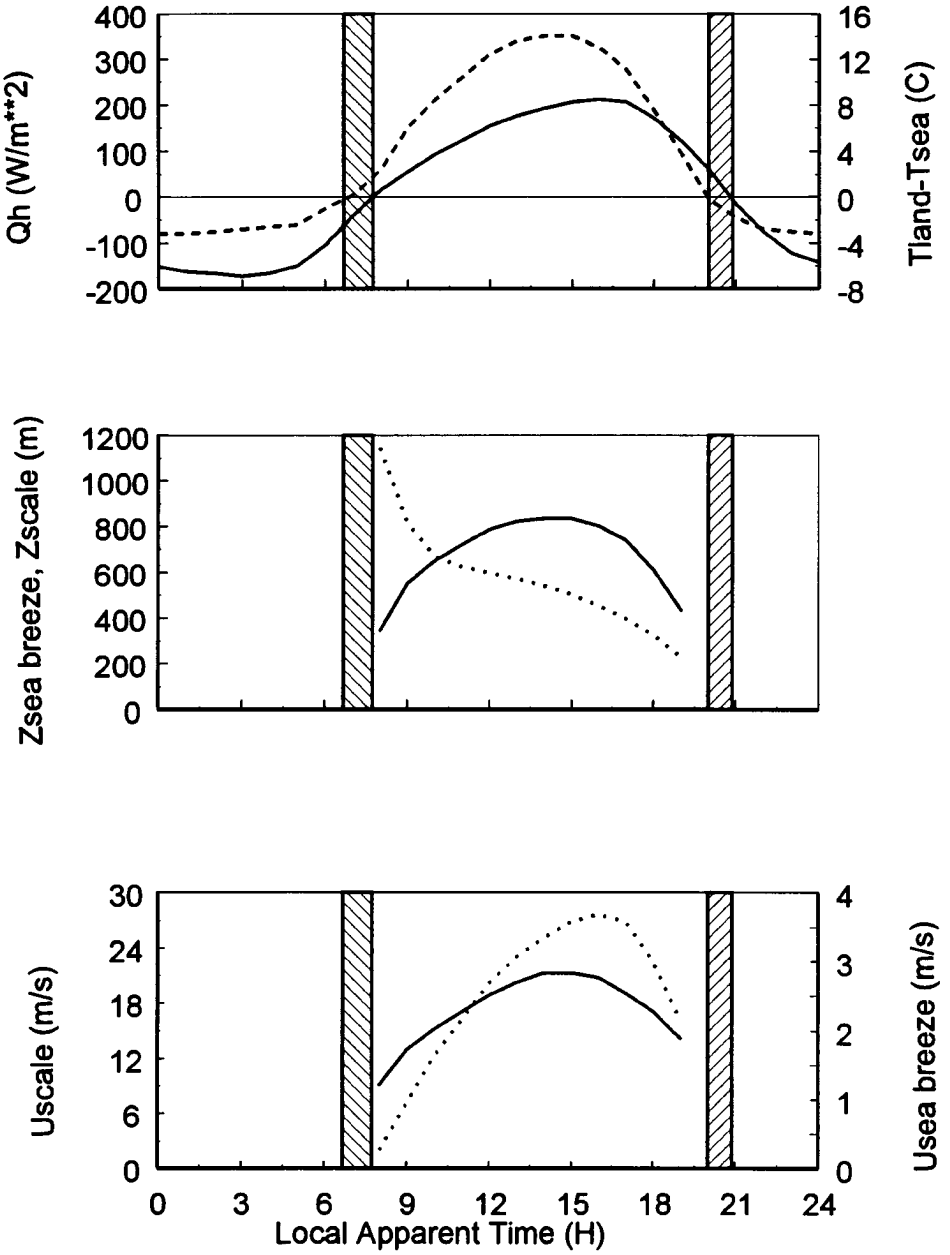

Figure 8. Top Panel: Diurnal evolution of surface-layer turbulent sensible heat flux density (dashed line) and land-sea temperature difference (solid line) as smoothed ensemble averages from all days in this study. Middle Panel: Diurnal evolution of sea-breeze length scale (dotted line) and sea-breeze depth (solid line) derived from top panel variables and scaling laws. Bottom Panel: Diurnal evolution of sea-breeze horizontal velocity (dotted line) and mean sea-breeze strength (solid line) derived from top panel variables and scaling laws. The shaded times indicate morning and afternoon transitions between land- and sea-breeze regimes, and correspond to times when heat flux and temperature difference have different signs.

to 2050 local apparent time in this case). Obviously the transitions will occur at different times, and have different duration on any given day, depending on the relative phase of these two forcing variables. In the illustrative case (as in most real cases), H leads ΔT. The middle panel shows that the resulting z_s initially has a large value, but quickly drops to a regime of steady decline through the day. The resultant sea breeze is initially shallow, but rises smoothly to a depth of roughly 800 m in mid afternoon, then declines again through the late afternoon. The lower panel shows how the sea-breeze horizontal velocity scale starts at zero after the morning transition period, grows rapidly to a maximum which coincides with the maximum land-sea temperature difference and then drops through the afternoon. The mean sea-breeze horizontal velocity rises slowly from a morning minimum to a broad maximum in mid afternoon. This picture of the evolution of a sea breeze is in accord with the host of observations made in many locations (Atkinson, 1981), and offers the advantage of very simple diagnostic estimates of the magnitude of the circulation from forcing variables.

4.3. A UNIVERSAL SEA-BREEZE PROFILE

The nondimensional sea-breeze profile is presented as a universal form, depending on no other external variables. It should therefore be applicable to sea breezes in all locations, other than those in which the sea-breeze circulation has significant interaction with topography. The only exception to this is the effect of surface friction. The present data reflect the effects of a relatively rough suburban surface with an estimated aerodynamic roughness length of 0.5 m. The resultant shear is likely to affect only the lowest portions of the profile. Obviously, the profile is only representative of conditions in which the synoptic wind is calm to light, and in opposition to the sea-breeze flow. This profile form can be used to validate results (when appropriately nondimensionalized) of mesoscale numerical models and analytical models of the sea-breeze circulation. A third-order polynomial approximating the universal profile is provided for this purpose.

Acknowledgements

I am grateful for field assistance from Keith Ayotte, Max Brown, Helen Cleugh, Sue Grimmond, Ian McKendry, Robert Nissen, Tim Oke, Hans-Peter Schmid, Tom Shalansky and Hu Wallis. Helen Cleugh provided turbulent sensible heat flux data from measurements made while working with Tim Oke. Dan Ciarniello, Nick Oke and Stephanie Smith performed the preliminary data analysis. Carol Evans of Environment Canada searched archived station and upper air data for me. I had fruitful discussions of the topic with Xiaoming Cai, Hiroshi Niino, Stewart Turner and Itsushi Uno. Funding for the research was from grants awarded by the Atmospheric Environment Service of Environment Canada and the Natural Science

and Engineering Research Council of Canada. The data were analyzed and paper written while I was a visiting Research Scientist at the Centre for Environmental Mechanics in Canberra and a Japan Society for the Promotion of Science Research Fellow at the National Institute for Environmental Studies, Tsukuba. Paul Jance drafted Figure 1.

References

Atkinson, B. W.: 1981, *Meso-scale Atmospheric Circulations*, Academic Press, 495 pp.

Cleugh, H. A. and Oke, T. R.: 1986, 'Suburban and Rural Energy Balance Comparisons in Summer for Vancouver, B.C.', *Boundary-Layer Meteorol.* **36**, 351–369.

Feliks, Y.: 1994, 'An Analytical Model of the Diurnal Oscillation of the Inversion Base Due to the Sea Breeze', *J. Atmos. Sci.* **51**, 991–998.

Finkele, K., Hacker, J. M., Kraus, H., and Scott, R. A. D.: 1995, 'A Complete Sea-breeze Circulation Cell Derived from Aircraft Observations', *Boundary-Layer Meteorol.* **73**, 299–317.

Fisher, E. L.: 1960, 'An Observational Study of the Sea Breeze', *J. Meteorol.* **17**, 645–660.

Hsu, S. A.: 1988, *Coastal Meteorology*, Academic Press, 260 pp.

Jehn, K. H.: 1973, *A Sea Breeze Bibliography 1664–1972*, Report No. 37, June 1973, Atmospheric Science Group, The University of Texas, College of Engineering, Austin, TX 78712, 57 pp.

Kimura, R. and Eguchi, T.: 1978, 'On the Dynamical Processes of Sea- and Land-Breeze Circulation', *J. Meteorol. Soc. Japan* **56**, 67–85.

Miao, Y. and Steyn, D. G.: 1995, 'Mesometeorological Modelling and Trajectory Studies during an Air Pollution Episode in the Lower Fraser Valley, B.C., Canada', in J. G. Watson, J. C. Chow, and P. A. Solomon (eds.), *Regional Photochemical Measurement and Modelling Studies*, Air and Waste Management Association, Pittsburgh, pp. 249–281.

Nakane, H. and Sasano, Y.: 1986, 'Structure of a Sea Breeze Front Revealed by a Scanning Lidar Observation', *J. Meteorol. Soc. Japan* **64**, 787–792.

Niino, H.: 1987, 'The Linear Theory of Land and Sea Breeze Circulation', *J. Meteorol. Soc. Japan* **65**, 901–920.

Oliphant, A. J.; 1996, *A Tropical Island Sea/Land Breeze System and its Interaction with Thunderstorm Activity, Northern Australia*, M.A. Thesis, University of Canterbury, Christchurch, 148 pp.

Rotunno, R.: 1983, 'On the Linear Theory of the Land and Sea Breeze', *J. Atmos. Sci.* **40**, 1999–2009.

Schmidt, F. H.: 1947, 'An Elementary Theory of the Land- and Sea-Breeze Circulation', *J. Meteorol.* **4**, 9–15.

Simpson, J. E.: 1994, *Sea Breeze and Local Winds*, Cambridge University Press, U.K., 234 pp.

Steyn, D. G. and Faulkner, D. A.: 1986, 'The Climatology of Sea-Breezes in the Lower Fraser Valley, BC', *Climatol. Bull.* **20**, 21–39.

Steyn, D. G.: 1997, 'Interaction Between the Internal Boundary Layer and Sea Breezes', in *Proceedings of EURSAP Workshop on The Determination of the Mixing Height: Current Progress and Problems*, Risø, Denmark, 1–3 October, 1997, pp. 137–140.

Ueda, H.: 1983, 'Effects of External Parameters on the Flow Field in the Coastal Region – A Linear Model', *J. Appl. Meteorol.* **22**, 312–321.

Walsh, J.: 1974, 'Sea Breeze Theory and Application', *J. Atmos. Sci.* **31**, 2012–2026.

Webster, I. and Farmer, D.: 1977, *Analysis of Lighthouse Station Temperature and Salinity Data – Phase II*. Institute of Ocean Sciences, Sidney, B.C., 93 pp.